Radiotherapy and Oncology 130 (2019) 149–155

Contents lists available at ScienceDirect

Radiotherapy and Oncology

journal homepage: www.thegreenjournal.com

Original article

Influence of volumetric modulated arc therapy and FET-PET scanning on treatment outcomes for glioblastoma patients

P. Munck af Rosenschold [a,b,*], I. Law [c], S. Engelholm [a], S.A. Engelholm [a], A. Muhic [a], M.J. Lundemann [a,b,c], H. Roed [a], K. Grunnet [a], H. Skovgaard Poulsen [a]

[a] Department of Oncology, Rigshospitalet, Copenhagen; [b] Niels Bohr Institute, University of Copenhagen; and [c] Department of Clinical Physiology, Nuclear Medicine and PET, Rigshospitalet, Copenhagen, Denmark

ARTICLE INFO

Article history:
Received 28 February 2017
Received in revised form 26 August 2018
Accepted 1 October 2018
Available online 13 November 2018

Keywords:
Glioblastoma
Radiotherapy
FET-PET
VMAT
IGRT
Technology

ABSTRACT

Background: We sought to assess the influence of the clinical introduction of new radiotherapy technologies on glioblastoma patients' outcomes.
Methods: Newly diagnosed glioblastoma patients treated with 60 Gy and temozolomide (2005–2014) were analyzed. The patients' GTV and CTV were defined based on MR ($n = 521$) or FET-PET/MR ($n = 190$), and were treated using conformal radiotherapy (CRT, $n = 159$) or image-guided volumetric modulated arc therapy with hippocampal sparing (IG-VMAT, $n = 362$). Progression-free survival (PFS) was assessed using the McDonald criteria. Associations between clinical data, dosimetry data, treatment technology, for PFS and overall survival (OS) were explored.
Results: The PFS (7 months) and OS (15 months) were unaffected by CRT, IG-VMAT and FET-PET technology. Mean brain dose was correlated with tumor volume, and was lower for IG-VMAT vs. CRT ($p < 0.001$). Larger mean brain dose was associated with inferior PFS (univariate/multivariate Cox models, $p < 0.001$) and OS (univariate, $p < 0.001$). Multivariate Cox models revealed association of larger mean brainstem dose ($p < 0.001$), BTV ($p = 0.045$), steroid use at baseline ($p = 0.003$), age ($p = 0.019$) and MGMT status ($p = 0.022$) with lower OS.
Conclusions: Introduction of hippocampal-sparing IG-VMAT technology appeared to be safe, and may have reduced toxicity and cognitive impairment. Larger mean brain dose was strongly associated with inferior PFS and OS.
 Radiotherapy and Oncology 130 (2019) 149–155

Glioblastomas are the most common primary brain tumor in adults. The median survival is only about 14–15 months despite combined surgery and chemo-radiotherapy [1]. Considerable technological advances have been made in the radiotherapy field [2], including IMRT [3], VMAT and IGRT[4], which have enabled high-precision radiotherapy [5,6], improved target dose conformity and reduction of radiation dose to selected organs at risk (OAR) [7–11]. In addition to the radiation delivery technology improvements, the use of amino acid-tracers such as ^{11}C-methionine (MET) and O-(2-^{18}F-flouroethyl)-L-tyrosine (FET) positron emission tomography (PET) for target definition of glioblastoma has recently been proposed and used in radiotherapy planning [12–15]. This notion has been prompted by studies showing that FET uptake correlates with tumor cell density and that FET-PET exhibit high specificity for glioma tissue [16,17]. Amino-acid tracers have been used for prediction of patterns of failure [18,19] and for prognostication of progression-free survival (PFS) and overall survival (OS) [20–22].

In our clinical practice, we have implemented IG-VMAT and FET-PET technology [23,24]. Our group has attempted FET-PET and MR-guided RT of recurrent glioma [25]. We have studied the recurrence pattern in relation to FET-PET and MR-scanning data [26], and constructed a prognostic model for treatment outcomes based on clinical characteristics [27]. The purpose of the current work was therefore to evaluate the influence on outcomes for glioblastoma patients by the introduction IG-VMAT and FET-PET scanning technology, in addition to the clinical characteristics found significant in ref. [27]. Further, we wished to evaluate the influence of the dose distribution on treatment outcomes.

Methods

Patients

We identified patients with histologically verified primary glioblastoma treated within the period 2005–2014. Patients eligi-

* Corresponding author at: Radiation Physics, Skåne University Hospital, Lund, Sweden.
E-mail address: per.munck@regionh.dk (P. Munck af Rosenschold).

https://doi.org/10.1016/j.radonc.2018.10.003
0167-8140/

ble for evaluation in this retrospective study were treated with radiotherapy to 60 Gy in 2 Gy-fractions with concomitant and adjuvant temozolomide (TMZ). TMZ was administered daily (75 mg/m^2) and subsequently in 6 cycles, for 5 days schedule every 28 days (150–200 mg/m^2). Histological evaluations were performed on formalin-fixed and paraffin-embedded tissue sample and graded using WHO guidelines. Further, O(6)-methylguanine-DNA methyltransferase (MGMT) protein status was determined using immunohistochemistry. Staining of more than 10% was considered positive for MGMT protein, and these patients were referred to as methylated in this work. Polymerase chain reaction (PCR) of MGMT promotor methylation status on the DNA level was not performed routinely. Previously, we have demonstrated a good inverse agreement between MGMT promotor methylation and MGMT protein status in a study, and therefore we find MGMT protein a reliable surrogate marker for the lack of MGMT promotor methylation [28]. All patients received either stereotactic biopsy or surgical resection before chemo-radiotherapy. Performance status was evaluated and graded (0–2) at the start of oncological treatment. Similarly, the use of steroid therapy was recorded at the start of oncological treatment. We dichotomized steroid use as phasing out (no use) if less than 15 mg/day, and (in use) if above 15 mg/day [22]. The patient data were prospectively collected: permission was granted by the Danish Data Protection Agency (2006-41-6979).

Imaging technology for radiotherapy planning

Patients were scanned using CT in the treatment position fixed using an aquaplastic mask system. A clinical spiral CT (Siemens) of the head was collected with 3-mm and subsequently (from 2012) 1-mm slice thickness (100 kVp, 400 mAs). A 1.5-Tesla MR-scanner (Siemens) was used to collect images post contrast injection (Gadovist, Bayer HealthCare). T1- and FLAIR/T2-weighted images were collected in the treatment position on a radiotherapy-dedicated scanner (from 2008). FET-PET/CT scanning was performed routinely from 2012. The FET-PET images had $0.8 \times 0.8 \times 3$ mm^3 voxels and were corrected for dead time, attenuation, randoms and scatter. Reconstruction of PET images was performed using ordered subset 3D expectation maximization (for details see [25]).

Delineation

The patients' imaging data were imported into the radiotherapy treatment planning software (iPlan, BrainLab AG, Germany and Eclipse, Varian Medical Systems) and the image series were co-registered. OAR were delineated on all image slices: eyes, optic nerves, optic chiasm, brainstem, whole brain, and also hippocampi (from 2009) The gross tumor volume (GTV) was defined using MR data as the contrast enhancing region and including the surgical cavity. Clinical target volume (CTV) was delineated by adding a 2-cm uniform margin to the GTV and then adjusted (reduced) to account for anatomical barriers such as bony structures, the brainstem and the tentorium. In order to account for set-up reproducibility during radiation treatment a planning target volume (PTV) margin was added to the CTV. Initially, the CTV-to-PTV margin was 5 mm, which was later reduced to 2 mm with the introduction of daily IG (from 2009 and onward). A Biological Target Volume (BTV) was defined using FET-PET scan data. The BTV was semi-automatically defined as the region with uptake equal to or greater than 1.6 times the background value [16]. Manual correction of the defined high uptake region was introduced by the nuclear medicine physician with reference to T1/T2 MRI, removing regions of reactive tissue and tissue with FET uptake not associated with the tumor. For the FET-PET scanned patient cohort, a combined MR-based GTV plus BTV volume was formed, and is referred to as the GTV hereafter.

Radiotherapy prescription

The patients all received the prescribed radiation dose of 60 Gy to the PTV. The brainstem, optic chiasm and nerves doses were nominally 54 Gy or less. However, for CRT patients the radiation dose coverage of the GTV and CTV was not compromised, causing the maximum dose to the brainstem and optic structures to exceed 54 Gy for some patients (see Fig. 1). Using VMAT, the maximum dose to the brainstem and the optic chiasm was kept below 54 Gy, though the max dose was 56–57 Gy to less than 1% of the volume occasionally. PRV:s were defined for the brainstem and was prioritized during optimization (max. dose of 56–57 Gy). For VMAT patients, the dose coverage of the CTV and the PTV was often compromised in favor of keeping the brainstem, optical chiasm and nerve doses below about 54 Gy. The doses to the eyes and the uninvolved brain were kept as low as possible. For VMAT patients, the hippocampi were contoured and the dosimetry prioritized above the uninvolved brain. We attempted to keep the bilateral hippocampi radiation dose D40 EQD2 less than about 7 Gy, which is based on Gondi et al. [8]. For the purpose of this analysis, we calculated the average dose to the brain as the dose delivered to the whole brain excluding the GTV (but including the CTV).

Radiotherapy technology

Patients treated 2005–2009: Radiotherapy was delivered using three-dimensional conformal radiotherapy (CRT, Table 1). The patients were set up using port radiographs at the start of the treatment. The tolerance used for the verification images was 5 mm. If the patient was outside of the tolerance, the patient's position was corrected and a new set of verification radiographs were acquired. The procedure was repeated until within tolerance. The verification procedure was repeated midway through the treatment. For the other treatment fractions the patients were set up using marks on the aqua-plastic mask.

Patients treated 2009–2012: Radiotherapy was delivered using Image-Guided hippocampal-sparing Volumetric Modulated Arc Therapy (IG-VMAT, Table 1). The daily IG protocol involved acquiring dual X-ray radiographs, which were compared with digitally reconstructed radiographs from the CT-scanning data, and were subsequently used to correct the patient's position. The tolerance of the verification images was 1 mm in all cardinal axis and 1 deg. rotation. If the patient was outside of the tolerance, the patient's position was corrected and a new set of verification radiographs were acquired. This procedure was repeated for each treatment field of each treatment fraction.

Patients treated 2012–2014: FET-PET/CT imaging was used in addition to MRI to define the target volume. Apart from the introduction of FET-PET scanning, the treatment procedure was otherwise unchanged as compared to the period 2009–2012 (PET-guided IG-VMAT, Table 1).

Statistics

The characteristics of the cohorts, CRT, IG-VMAT and PET-guided IG-VMAT, were compared using Kruskal–Wallis or Chi-squared tests. The progression free survival (PFS) and overall survival (OS) were calculated using the Kaplan–Meier method, and the three cohorts were compared using log rank statistics. Univariate and multivariate Cox models for PFS and OS were constructed based on clinical data, technology use and dosimetric data for the whole cohort. In the univariate models a Bonferroni corrected p-value of 0.004 or less was considered significant, while a p-value

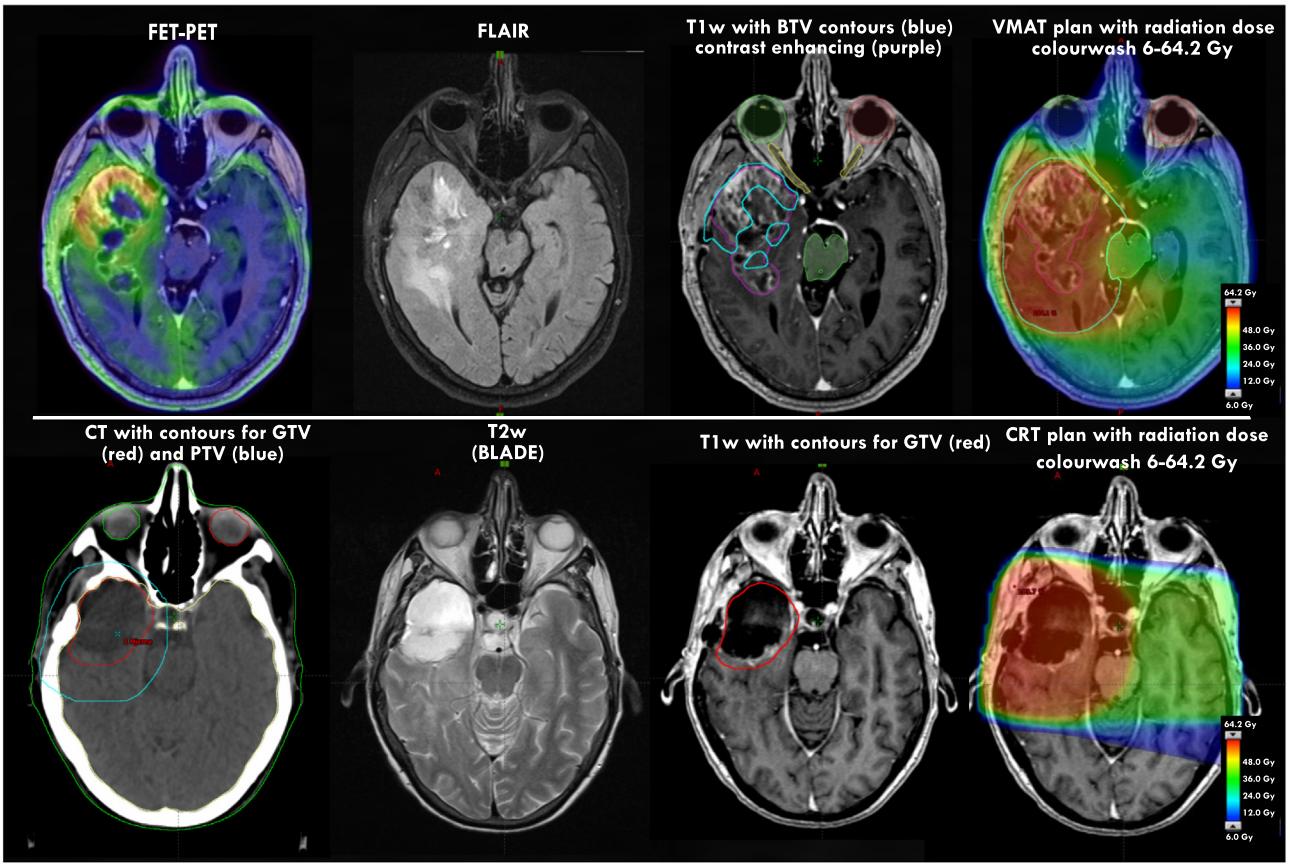

Fig. 1. FET-PET/CT and MR-scanned patient treated with IG-VMAT (top row) and a CT/MR-scanned patient treated with CRT (bottom row).

Table 1
Patient characteristics.

Patient characteristics		CRT (2005–2009)		IG-VMAT (2009–2012)		PET-IG-VMAT (2012–2014)			
Parameter		Count	Median (min-max)	Count	Median (min-max)	Count	Median (min-max)	Statistic	*p*-value
Number of patients		159		172		190			
MGMT protein status	Unmethylated	42		93		111		Chi-square	0.003
	Methylated	52		56		58			
Age			58 (22–75)		62 (23–76)		61 (31–79)	Kruskal-Wallis	0.003
Steroid use	No	56		81		94		Chi-square	0.027
	Yes	101		91		96			
Perf. status	0	96		110		105		Kruskal-Wallis	0.243
	1	40		57		74			
	2	17		5		10			
GTV total cc			60.7 (2.9–269.5)		37.0 (3–186.9)		38.2 (2.1–235.6)	Kruskal-Wallis	<0.001
BTV PET cc							19.8 (0.0–190.3)	N/A	
Brain, mean dose [Gy]			33.1 (10.9–46.9)		27.6 (11.0–46.6)		26.0 (9.0–44.0)	Kruskal-Wallis	<0.001
Brainstem, mean dose [Gy]			21.5 (3.2–60.0)		27.2 (0.6–52.9)		21.6 (0.4–44.5)	Kruskal-Wallis	0.052
Hippoc. L, mean dose [Gy]					24.5 (0.7–62.0)		13.3 (0.6–60.7)	Mann-Whitney	0.052
Hippoc. R, mean dose [Gy]					28.5 (1.0–60.7)		11.2 (0.5–62)	Mann-Whitney	0.068
D95 (GTV) [Gy]			59.5 (55.5–61.7)		59.0 (55.1–61.4)		59.0 (54.5–61.1)	Kruskal-Wallis	<0.001
PFS, median (years)			0.58 (0.17–10.8)		0.58 (0.08–6.08)		0.50 (0.17–4.0)		
PFS events		156		165		178			
OS, median (years)			1.17 (0.25–10.8)		1.25 (0.08–6.08)		1.25 (0.17–4.0)		
Death events		155		152		150			

of 0.05 was considered a trend. A forward selection process was used for the multivariate model, where covariates with *p*-values of 0.1 or less could enter the model and covariates with *p*-values less than 0.05 were kept in the final model. For the multivariate models, a bootstrapping procedure with 10,000 samples drawn with replacement was used to evaluate the uncertainty of the model. The correlation between significant covariates in the full Cox model was explored using Spearman signed ranks statistics. Finally, the patient cohort was split into a favorable and an unfavorable group based on the median survival function obtained from the Cox model, and the Kaplan–Meier estimates of PFS and OS was plotted and compared using log rank statistics. Calculations were performed using SPSS (v24, IBM, US) and R (version 3.3.2). Multiple linear regression models were used to explore associations between mean brain dose, treatment technology (IG-VMAT vs. CRT), and GTV size.

Results

The information regarding the use of radiotherapy technology as well as the radiotherapy records was lacking for 13 patients; these were excluded from further analysis. A total of 521 patients were found to be evaluable and included in the analysis. The characteristics of the patients can be found in Table 1. Two cases of radiotherapy plans are shown in Fig. 1.

The PFS and the OS were similar for patients treated with CRT, IG-VMAT and PET-Guided IG-VMAT (non-significant log rank test). However, the comparison is not straightforward given that the baseline characteristics of the three cohorts were dissimilar. The CRT cohort had a larger fraction of methylated tumors ($p = 0.003$), was younger ($p = 0.003$), had larger fraction of patients on steroids ($p = 0.027$) and had larger GTVs ($p < 0.001$).

The Cox model data are reported in Tables 2 (PFS) and 3 (OS). For PFS, PS, steroid use, GTV size, BTV size, and the mean brain dose were all significant univariately, while only mean brain dose remained significant in the multivariate model. For OS, MGMT status, age, PS, steroid use, GTV size, BTV size and mean dose to brain and brainstem were significant univariately. In the multivariate model, MGMT status, age, steroid use, GTV size, BTV size and mean dose to the brainstem were significantly contributing to the model ($p < 0.05$). Bootstrap analysis revealed that both the multivariate Cox models were robust, and p-values reported remained significant and were all within 0.005 of those reported in Tables 2 and 3. The Cox model was verified and reproduced using the R software, where Martingale, Schoenfeld and deviance residuals were examined.

The inclusion of radiotherapy treatment technique (IG-VMAT vs. CRT) and FET-PET-guided vs. MR only target definition was non-significant in the Cox models for PFS and OS. Interestingly, the radiation dose received by 95% of the GTV (D95), which is a measure of the target dose coverage, was trending toward significance with a hazard ratio of 0.859 ($p = 0.008$) for OS.

Patients were split into two groups based on the Cox models median survival function, and are referred to as "Favorable" and "Unfavorable" based on their prognosis. Favorable and Unfavorable groups were formed using the Cox model for both PFS and OS. Subsequently, Kaplan–Meier estimates for the favorable and unfavorable groups for both PFS and OS were calculated and are presented in Fig. 2A–C.

Most of the prognostic factors were internally correlated, notably the use of steroids and the performance status at the start of oncologic treatment, GTV size, BTV size and mean brain dose (rho > 0.15, $p < 0.01$). Further, the mean dose to the brainstem was correlated to the hippocampi doses (rho > 0.5, $p < 0.001$), the mean dose to the whole brain (rho = 0.52, $p < 0.001$) and worse dose coverage of the GTV (GTV D95) (rho = −0.27, $p < 0.001$). Finally, multiple linear regression models revealed that increased mean brain dose was associated with both GTV size and use of CRT ($p < 0.001$). Thus, for patients with equivalent GTV size the use of IG-VMAT technology produced radiation dose distributions with lower mean brain dose than CRT.

Discussion

To our knowledge, this is the first report to demonstrate strong association of mean brain dose delivered and PFS and OS of glioblastoma patients. The association of larger dose to the brain and inferior PFS and OS is present in the univariate Cox regression models and outcomes data for 475 glioblastoma patients, as well as the smaller cohort of 163 patients evaluable using the multivariate Cox model for PFS. Interestingly, in the multivariate Cox model for PFS, the mean brain dose remained significant, while well-established prognostic factors such as performance status were not. For OS, the multivariate Cox model for 163 patients included MGMT status, age at therapy, steroid use at baseline (yes/no), BTV size, which are well-known prognostic factors, but also mean dose to the brainstem was significantly associated with OS.

We found no statistically significant difference in the PFS or OS outcomes after the clinical introduction of IG-VMAT or FET-PET-guided radiotherapy planning. Given that IG and VMAT were introduced simultaneously, we have no means of separating any potential clinical impact of either, but must look at the combined effect. With respect to VMAT, the technique allows for improved dose conformity with steep dose gradients toward the uninvolved brain tissue, compared to CRT. Concurrently, with the introduction of daily IG we introduced narrower PTV margins by merit of the smaller positioning uncertainty, which allowed for greater dose conformity around the target [6]. One could envision an increased risk of recurrences in the rim of the CTV due to the greater dose conformity intrinsic to IG-VMAT with narrower PTV margins as compared to CRT without daily IG and wide PTV margins. Given unchanged PFS and OS, we consider this unsupported by our data. While multiple linear regression revealed that IG-VMAT produced statistically significant lower mean dose to the brain than CRT (similar to other authors [29–31]), the difference was numerically too small to impact PFS or OS outcomes, which is contrary to [29]

Table 2
Univariate and multivariate Cox models for progression-free survival. Bootstrapping revealed that all the 95% confidence interval of the p-values of the multivariate model is within 0.005 of those reported below. Significant covariates are printed in bold typeface and trends are italicized.

Univariate Cox models: progression-free survival					Multivariate Cox model: progression-free survival		
Parameter	n	HR	p-value		n	HR	p-value
Overall model					163		**<0.001**
MGMT Protein Status	412	1.224	0.051				
Age	*521*	*1.010*	*0.021*				
PS at start of oncologic therapy	**514**	**1.294**	**<0.001**				
Steroids	**519**	**1.377**	**<0.001**				
CRT vs VMAT w hippocampal sparing	521	1.065	0.513	ref = VMAT			
MR vs FET	521	1.071	0.463	ref = MR			
GTV total (cc)	**482**	**1.004**	**0.001**				
BTV PET (cc)	**190**	**1.009**	**<0.001**				
Tumor dose conformity, GTV D95 (Gy)	485	0.905	0.074				
Mean brain dose (Gy)	**474**	**1.036**	**<0.001**			**1.060**	**<0.001**
Mean brainstem dose (Gy)	*365*	*1.010*	*0.009*				
Mean hippocampus dose L (Gy)	356	1.004	0.064				
Mean hippocampus dose R (Gy)	*355*	*1.005*	*0.036*				

Table 3
Univariate and multivariate Cox models for overall survival. Bootstrapping revealed that all the 95% confidence interval of the reported *p*-values of the multivariate model is within 0.005 of those reported. Significant covariates are printed in bold typeface and trends are italicized.

Univariate Cox models: overall survival					Multivariate Cox model: overall survival		
Parameter	n	HR	*p*-value		n	HR	*p*-value
Overall model					163		**<0.001**
MGMT Protein Status	**412**	**1.542**	**<0.001**			**1.541**	**0.022**
Age (years)	**521**	**1.022**	**<0.001**			**1.023**	**0.019**
PS at start of oncologic therapy	**514**	**1.591**	**<0.001**				
Steroids	**519**	**1.776**	**<0.001**			**1.755**	**0.003**
CRT vs VMAT w hippocampal sparing	521	0.918	0.394	ref = VMAT			
MR vs FET	521	0.905	0.638	ref = MR			
GTV total cc	**482**	**1.003**	**0.002**				
BTV PET cc	**190**	**1.008**	**<0.001**			**1.006**	**0.045**
Tumor dose conformity, GTV D95 (Gy)	*485*	*0.859*	*0.008*				
Mean brain dose (Gy)	**474**	**1.043**	**<0.001**				
Mean brainstem dose (Gy)	**365**	**1.014**	**0.001**			**1.031**	**<0.001**
Mean hippocampus dose L (Gy)	*356*	*1.006*	*0.015*				
Mean hippocampus dose R (Gy)	355	1.003	0.174				

where, however, the dissimilar histology of the VMAT and CRT cohorts may obscure the sole impact of technology.

Given the correlation of FET-PET uptake with tumor cell density [16,17], the use of FET-PET in the target delineation for RT should, at least in theory, improve the radiation dose coverage of infiltrative disease. However, we observe no change in either PFS or OS with the introduction of routine FET PET scanning as part of the radiotherapy planning workup. A potential reason for the similar outcomes after introduction of FET-PET scanning could be that the solely MRI-based target definition encompasses the BTV for most patients [23,32]. Consistent with several previous studies, we find that increased pre-treatment post-surgical amino acid-based PET BTV size is a prognostic marker associated with inferior OS [20,33–35].

A major finding in this analysis is the very strong association of large mean brain dose and inferior PFS and OS. This immediately suggests that large volume of brain tissue irradiated to a high dose may impact the toxicity of the treatment as well as the PFS, which appears consistent with the recent QUANTEC report [9]. The association of mean brain dose with PFS and OS should be interpreted with caution. First, the factors associated with poor prognosis were internally correlated, in particular GTV size and mean brain dose ($p < 0.01$). The gross tumor size (i.e. the GTV) is affecting the size of the CTV (equal to the GTV plus up to 2 cm) that defined during the radiotherapy planning process, which is (unsurprisingly) correlated to the mean brain dose. In addition, it is most likely such that localization of the target volume will affect the mean brain dose: a centrally located target must tend to have larger mean brain dose than a peripheral target. The localization of the primary tumor appears related to the glioblastoma phenotype [36]. Our data support lowering the dose to the hippocampi, given the association with improved cognition outcomes [8] and the inferior PFS and/or OS with increased dose in this data set (borderline statistically significant). Poor radiation dose coverage of the GTV is due to prioritizing the OAR dose over tumor coverage in the planning process. Interestingly, poor tumor radiation dose coverage (GTV D95) was borderline statistically significant ($p = 0.008$) associated with inferior OS, suggesting that poor radiation dose coverage of the GTV may be detrimental to the survival of the patient. Alternatively, a centrally located tumor (close to the brainstem) is a poor prognostic factor and that the mean dose to the brainstem is a surrogate of localization, or a combination of these two effects.

The overall survival match of our complete cohort was fairly similar to the chemo-radiation arm of the seminal Stupp et al publication (Fig. 2). The survival difference in the favorable and unfavorable cohorts in the plots in Fig. 2 amount to approximately 3 and 8 months for median PFS and OS, respectively, when based on the mean brain dose. This survival difference in the plots in Fig. 2A–C exceeded the benefit in survival found by the introduction of temozolomide (approximately 2 months), though this observation should be interpreted with great caution: the cohorts in this work were retrospectively split based on prognostic factors. We note also that the survival curves in Fig. 2B eventually join, and that lasting survival for GBM patients was very modest, and limited to a few percent at 5 years. Though based on fewer patients and with shorter follow-up, a stronger separation of the survival curves was obtained by making use of the full Cox model (Fig. 2C).

There are several limitations to the present study, primarily due to its retrospective nature. Given that the treatment technology was introduced for all patients for a certain time-period, we do not believe there was selection bias in our data. However, we acknowledge the fact that the time from diagnosis to treatment, not all data were known for all patients, and salvage therapy practices may have varied for the period. Our group recently identified a subgroup of recurrent GBM patients benefitting from bevacizumab therapy [37], though this appears to have limited impact on the overall survival of the cohort. Further, the subventricular zone was not routinely contoured, which has been shown to be associated to the patterns of failure and survival [38–40]. In addition, we note a curious imbalance of the distribution of MGMT status (see Table 1) of the three cohorts, which might obscure the impact of technology in this evaluation. The premise of the current work was to base the investigation on technology impact on patient outcomes on our group's previous findings regarding the significant clinical characteristics [27]. The associations of PFS and OS with radiation dosimetry metrics, the tumor localization and size, imaging features in MR and FET PET data sets, and clinical prognostic factors such as the extent of surgery for glioblastoma patients treated with surgery and radio-chemotherapy warrant further studies, which is however beyond the scope of the current work. The use of reduced GTV-to-CTV margins [26,41–44] and/or of proton therapy [24,45] may be of interest for further study given that these are potential methods for reducing the mean brain dose.

In conclusion, we find that the introduction of highly conformal hippocampal-sparing IG-VMAT has been safe and have reduced the dose to the uninvolved brain and to the hippocampi without deteriorating the progression free or overall survival. Interestingly, we find that the mean brain dose was very strongly associated with both inferior PFS and OS, which should be considered in designing future radiotherapy protocols.

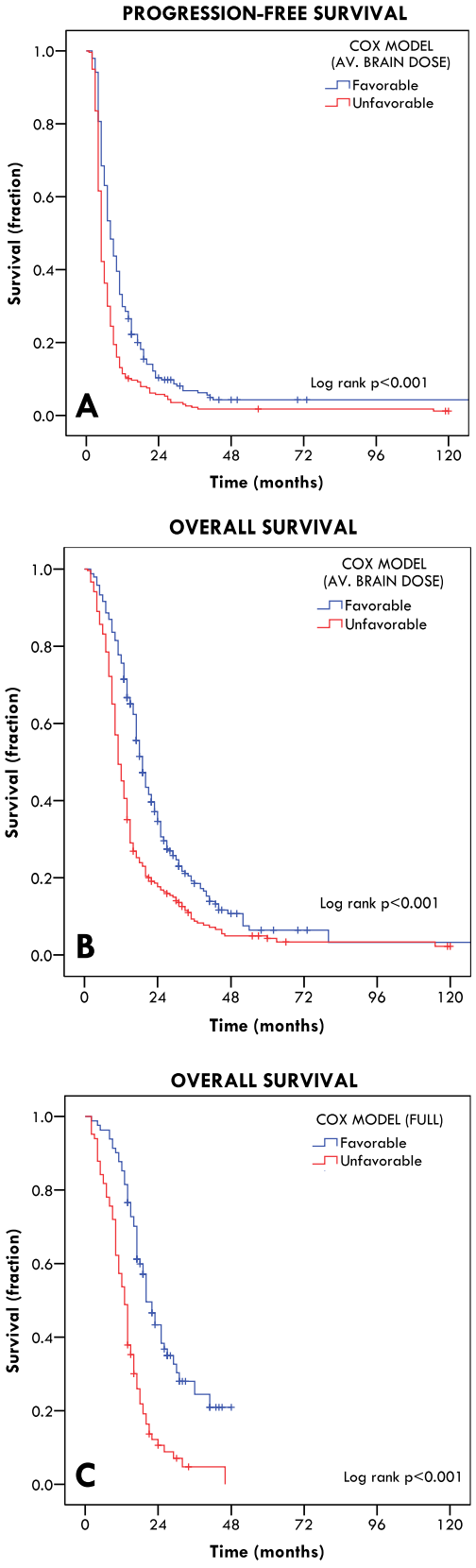

Fig. 2. A–C: Progression-free survival (A) and Overall survival for the cohort (B–C). The cohort has been split into a "Unfavorable" group with a survival function less than median and a "Favorable" group with higher than the median survival function, as calculated based on the mean brain dose (A–B) or the full multivariate model for OS (C).

Conflict of interest

Nothing to disclose.

Funding

The Lundbeck Foundation is acknowledged for financial support.

Acknowledgement

Katrin Håkansson MSc and Copenhagen statistics unit (University of Copenhagen, Denmark) are acknowledged for valuable discussions.

References

[1] Stupp R, Mason WP, van den Bent MJ, Weller M, Fisher B, Taphoorn MJ, et al. European Organisation for R, Treatment of Cancer Brain T, Radiotherapy G, National Cancer Institute of Canada Clinical Trials G. Radiotherapy plus concomitant and adjuvant temozolomide for glioblastoma. New England J Med 2005;352:987–96.
[2] Gzell C, Back M, Wheeler H, Bailey D, Foote M. Radiotherapy in glioblastoma: the past, the present and the future. Clin Oncol (R Coll Radiol) 2016.
[3] Brahme A, Roos JE, Lax I. Solution of an integral equation encountered in rotation therapy. Phys Med Biol 1982;27:1221–9.
[4] Verellen D, De Ridder M, Linthout N, Tournel K, Soete G, Storme G. Innovations in image-guided radiotherapy. Nat Rev Cancer 2007;7:949–60.
[5] Tarnavski N, Engelholm SA, Munck Af Rosenschold P. Fast intra-fractional image-guidance with 6D positioning correction reduces delivery uncertainty for stereotactic radiosurgery and radiotherapy. J Radiosurg SBRT 2015;4:15–20.
[6] van Herk M, Remeijer P, Rasch C, Lebesque JV. The probability of correct target dosage: dose-population histograms for deriving treatment margins in radiotherapy. Int J Radiat Oncol Biol Phys 2000;47:1121–35.
[7] Adeberg S, Harrabi SB, Bougatf N, Bernhardt D, Rieber J, Koerber SA, et al. Intensity-modulated proton therapy, volumetric-modulated arc therapy, and 3D conformal radiotherapy in anaplastic astrocytoma and glioblastoma: a dosimetric comparison. Strahlentherapie und Onkologie: Organ der Deutschen Rontgengesellschaft [et al] 2016;192:770–9.
[8] Gondi V, Hermann BP, Mehta MP, Tome WA. Hippocampal dosimetry predicts neurocognitive function impairment after fractionated stereotactic radiotherapy for benign or low-grade adult brain tumors. Int J Radiat Oncol Biol Phys 2013;85:348–54.
[9] Lawrence YR, Li XA, el Naqa I, Hahn CA, Marks LB, Merchant TE, et al. Radiation dose-volume effects in the brain. Int J Radiat Oncol Biol Phys 2010;76(3 Suppl): S20–7.
[10] Mayo C, Martel MK, Marks LB, Flickinger J, Nam J, Kirkpatrick J. Radiation dose-volume effects of optic nerves and chiasm. Int J Radiat Oncol Biol Phys 2010;76 (3 Suppl):S28–35.
[11] Mayo C, Yorke E, Merchant TE. Radiation associated brainstem injury. Int J Radiat Oncol Biol Phys 2010;76(3 Suppl):S36–41.
[12] Grosu AL, Weber WA. PET for radiation treatment planning of brain tumours. Radiother Oncol: J Eur Soc Therap Radiol Oncol 2010;96:325–7.
[13] Niyazi M, Geisler J, Siefert A, Schwarz SB, Ganswindt U, Garny S, et al. FET-PET for malignant glioma treatment planning. Radiother Oncol: J Eur Soc Therap Radiol Oncol 2011;99:44–8.
[14] Weber DC, Zilli T, Buchegger F, Casanova N, Haller G, Rouzaud M, et al. [(18)F] Fluoroethyltyrosine- positron emission tomography-guided radiotherapy for high-grade glioma. Radiat Oncol 2008;3:44.
[15] Grosu AL, Nestle U, Weber WA. How to use functional imaging information for radiotherapy planning. Eur J Cancer 2009;45(Suppl 1):461–3.
[16] Pauleit D, Floeth F, Hamacher K, Riemenschneider MJ, Reifenberger G, Muller HW, et al. O-(2-[18F]fluoroethyl)-L-tyrosine PET combined with MRI improves the diagnostic assessment of cerebral gliomas. Brain 2005;128:678–87.
[17] Stockhammer F, Plotkin M, Amthauer H, van Landeghem FK, Woiciechowsky C. Correlation of F-18-fluoro-ethyl-tyrosin uptake with vascular and cell density in non-contrast-enhancing gliomas. J Neurooncol 2008;88:205–10.
[18] Lee IH, Piert M, Gomez-Hassan D, Junck L, Rogers L, Hayman J, et al. Association of 11C-methionine PET uptake with site of failure after concurrent temozolomide and radiation for primary glioblastoma multiforme. Int J Radiat Oncol Biol Phys 2009;73:479–85.
[19] Weber DC, Casanova N, Zilli T, Buchegger F, Rouzaud M, Nouet P, et al. Recurrence pattern after [(18)F]fluoroethyltyrosine-positron emission tomography-guided radiotherapy for high-grade glioma: a prospective study. Radiother Oncol: J Eur Soc Therap Radiol Oncol 2009;93:586–92.
[20] Piroth MD, Holy R, Pinkawa M, Stoffels G, Kaiser HJ, Galldiks N, et al. Prognostic impact of postoperative, pre-irradiation (18)F-fluoroethyl-l-tyrosine uptake in glioblastoma patients treated with radiochemotherapy. Radiother Oncol: J Eur Soc Therap Radiol Oncol 2011;99:218–24.

[21] Piroth MD, Pinkawa M, Holy R, Klotz J, Nussen S, Stoffels G, et al. Prognostic value of early [18F]fluoroethyltyrosine positron emission tomography after radiochemotherapy in glioblastoma multiforme. Int J Radiat Oncol Biol Phys 2011;80:176–84.
[22] Poulsen SH, Urup T, Grunnet K, Christensen IJ, Larsen VA, Jensen ML, et al. Law I. The prognostic value of FET PET at radiotherapy planning in newly diagnosed glioblastoma. Eur J Nucl Med Mol Imaging 2016.
[23] Munck af Rosenschold P, Costa J, Engelholm SA, Lundemann MJ, Law I. Impact of [18F]-fluoro-ethyl-tyrosine PET imaging on target definition for radiation therapy of high-grade glioma. Neuro-Oncology 2015;17:757–63.
[24] Munck af Rosenschold P, Engelholm S, Ohlhues L, Law I, Vogelius I, Engelholm SA. Photon and proton therapy planning comparison for malignant glioma based on CT, FDG-PET, DTI-MRI and fiber tracking. Acta Oncol 2011;50:777–83.
[25] Moller S, Law I, Munck Af Rosenschold P, Costa J, Poulsen HS, Engelholm SA, et al. Prognostic value of 18F-FET PET imaging in re-irradiation of high-grade glioma: results of a phase I clinical trial. Radiother Oncol: J Eur Soc Therap Radiol Oncol 2016;121:132–7.
[26] Lundemann M, Costa JC, Law I, Engelholm SA, Muhic A, Poulsen HS, et al. Patterns of failure for patients with glioblastoma following O-(2-[18F] fluoroethyl)-L-tyrosine PET- and MRI-guided radiotherapy. Radiother Oncol: J Eur Soc Therap Radiol Oncol 2017.
[27] Michaelsen SR, Christensen IJ, Grunnet K, Stockhausen MT, Broholm H, Kosteljanetz M, et al. Clinical variables serve as prognostic factors in a model for survival from glioblastoma multiforme: an observational study of a cohort of consecutive non-selected patients from a single institution. BMC Cancer 2013;13:402.
[28] Kristensen LS, Michaelsen SR, Dyrbye H, Aslan D, Grunnet K, Christensen IJ, et al. Assessment of quantitative and allelic MGMT methylation patterns as a prognostic marker in glioblastoma. J Neuropathol Exp Neurol 2016;75:246–55.
[29] Navarria P, Pessina F, Cozzi L, Ascolese AM, Lobefalo F, Stravato A, et al. Can advanced new radiation therapy technologies improve outcome of high grade glioma (HGG) patients? Analysis of 3D-conformal radiotherapy (3DCRT) versus volumetric-modulated arc therapy (VMAT) in patients treated with surgery, concomitant and adjuvant chemo-radiotherapy. BMC Cancer 2016;16:362.
[30] Narayana A, Yamada J, Berry S, Shah P, Hunt M, Gutin PH, et al. Intensity-modulated radiotherapy in high-grade gliomas: clinical and dosimetric results. Int J Radiat Oncol Biol Phys 2006;64:892–7.
[31] Wagner D, Christiansen H, Wolff H, Vorwerk H. Radiotherapy of malignant gliomas: comparison of volumetric single arc technique (RapidArc), dynamic intensity-modulated technique and 3D conformal technique. Radiother Oncol: J Eur Soc Therap Radiol Oncol 2009;93:593–6.
[32] Rieken S, Habermehl D, Giesel FL, Hoffmann C, Burger U, Rief H, et al. Analysis of FET-PET imaging for target volume definition in patients with gliomas treated with conformal radiotherapy. Radiother Oncol: J Eur Soc Therap Radiol Oncol 2013;109:487–92.
[33] Poulsen SH, Urup T, Grunnet K, Christensen IJ, Larsen VA, Jensen ML, et al. The prognostic value of FET PET at radiotherapy planning in newly diagnosed glioblastoma. Eur J Nucl Med Mol Imaging 2016.
[34] Jansen NL, Suchorska B, Wenter V, Schmid-Tannwald C, Todica A, Eigenbrod S, et al. Prognostic significance of dynamic 18F-FET PET in newly diagnosed astrocytic high-grade glioma. J Nucl Med: Official Publ, Soc Nucl Med 2015;56:9–15.
[35] Suchorska B, Jansen NL, Linn J, Kretzschmar H, Janssen H, Eigenbrod S, et al. Biological tumor volume in 18FET-PET before radiochemotherapy correlates with survival in GBM. Neurology 2015;84(7):710–9.
[36] Ellingson BM, Lai A, Harris RJ, Selfridge JM, Yong WH, Das K, et al. Probabilistic radiographic atlas of glioblastoma phenotypes. AJNR Am J Neuroradiol 2013;34:533–40.
[37] Urup T, Michaelsen SR, Olsen LR, Toft A, Christensen IJ, Grunnet K, et al. Angiotensinogen and HLA class II predict bevacizumab response in recurrent glioblastoma patients. Mol Oncol 2016;10:1160–8.
[38] Lim DA, Cha S, Mayo MC, Chen MH, Keles E, VandenBerg S, et al. Relationship of glioblastoma multiforme to neural stem cell regions predicts invasive and multifocal tumor phenotype. Neuro-Oncology 2007;9:424–9.
[39] Jafri NF, Clarke JL, Weinberg V, Barani IJ, Cha S. Relationship of glioblastoma multiforme to the subventricular zone is associated with survival. Neuro-oncology 2013;15:91–6.
[40] Lee P, Eppinga W, Lagerwaard F, Cloughesy T, Slotman B, Nghiemphu PL, et al. Evaluation of high ipsilateral subventricular zone radiation therapy dose in glioblastoma: a pooled analysis. Int J Radiat Oncol Biol Phys 2013;86:609–15.
[41] McDonald MW, Shu HK, Curran Jr WJ, Crocker IR. Pattern of failure after limited margin radiotherapy and temozolomide for glioblastoma. Int J Radiat Oncol Biol Phys 2011;79:130–6.
[42] Paulsson AK, McMullen KP, Peiffer AM, Hinson WH, Kearns WT, Johnson AJ, et al. Limited margins using modern radiotherapy techniques does not increase marginal failure rate of glioblastoma. Am J Clin Oncol 2014;37:177–81.
[43] Gebhardt BJ, Dobelbower MC, Ennis WH, Bag AK, Markert JM, Fiveash JB. Patterns of failure for glioblastoma multiforme following limited-margin radiation and concurrent temozolomide. Radiat Oncol 2014;9:130.
[44] Minniti G, Amelio D, Amichetti M, Salvati M, Muni R, Bozzao A, et al. Patterns of failure and comparison of different target volume delineations in patients with glioblastoma treated with conformal radiotherapy plus concomitant and adjuvant temozolomide. Radiother Oncol 2010;97:377–81.
[45] Harrabi SB, Bougatf N, Mohr A, Haberer T, Herfarth K, Combs SE, et al. Dosimetric advantages of proton therapy over conventional radiotherapy with photons in young patients and adults with low-grade glioma. Strahlenther Onkol 2016;192:759–69.